



Effect of applied standard wood machining fluid on colour and chemical composition of the machined wood surface

Daniel Chuchala¹ · Agata Sommer² · Kazimierz A. Orłowski¹ · Hanna Staroszczyk² · Szymon Mania³ · Jakub Sandak^{4,5}

Received: 23 March 2023 / Accepted: 22 August 2023
© The Author(s) 2023

Abstract

Appropriate monitoring of wood machining processes is a key issue to ensure the expected quality of the processed wood, expected efficiency and minimize energy consumption of production processes. A new trend is the design of environmentally friendly machining fluids. In this paper, as a preliminary study in this field, the effect of applied standard wood machining fluid on changes in the colour and chemical composition of the machined wood surface is presented. Scots pine wood (*Pinus sylvestris* L.) was used for this research. Colour measurements were carried out based on the three-axis CIELab system test in time intervals and coefficients such as: colour chroma (C_{ab}^*), colour saturation (S_{ab}^*), colour hue (h°), and total colour changes (ΔE^*). Changes in chemical composition were analysed on the Attenuated Total Reflectance Fourier Transform Infrared Spectroscopy (ATR FT-IR). The results confirmed that standard machining fluids cause a significant change in the colour of the treated pine surface, which decreases over time but is still present even after 24 h. For the spectral analysis, no chemical changes were observed between the machining fluid and the wood. However, the fluid particles remained in the wood after 24 h. In order to reduce the effect of the machining fluid on the colour of the wood, its composition should be changed to allow and/or accelerate the evaporation of their components from the treated wood surface.

1 Introduction

Wood is a natural and renewable biological material with optimal functional properties (Asdrubali et al. 2017). These properties allow for wood to be widely used in civil engineering (Ramage et al. 2017; Wieruszewski and Mazela 2017), architecture (Sekularac et al. 2016), and the furniture industry (Wu et al. 2021). The good mechanical properties, low density, and easy harvesting are features that compete with mineral-based building materials such as concrete or

steel (Hassan and Johansson 2018). Hence, wood is widely used even in the construction of skyscrapers (Harris 2012; Tollefson 2017). Wood is also a competitive material due to its much lower carbon footprint compared to traditional building materials (Himes and Busby 2020). The above mentioned features and its renewability place wood in a leading position among materials used in construction. Wood and its application in civil engineering is also seen as one of the most important tools for carbon storage, especially

✉ Daniel Chuchala
daniel.chuchala@pg.edu.pl

Agata Sommer
agata.sommer@pg.edu.pl

Kazimierz A. Orłowski
kazimierz.orłowski@pg.edu.pl

Hanna Staroszczyk
hanna.staroszczyk@pg.edu.pl

Szymon Mania
szymon.mania@pg.edu.pl

Jakub Sandak
jakub.sandak@innorenew.eu

¹ Faculty of Mechanical Engineering and Ship Technology and EkoTech Center, Gdansk University of Technology, Gabriela Narutowicza 11/12, Gdansk, Poland

² Faculty of Chemistry and EkoTech Center, Gdansk University of Technology, Gabriela Narutowicza 11/12, Gdansk, Poland

³ Faculty of Chemistry and Advanced Materials Center, Gdansk University of Technology, Gabriela Narutowicza 11/12, Gdansk, Poland

⁴ InnoRenew CoE, Livade 6a, 6310 Izola, Slovenia

⁵ Andrej Marušič Institute, University of Primorska, Muzejski Trg 2, 6000 Koper, Slovenia

as a recommended solution for mitigating climate change (Tetty et al. 2019; Brunet-Navarro et al. 2021).

The natural features of wood, including knots, sorption properties, and shape stability, reduce the values of mechanical properties, and as a result, hinder its wider use (As et al. 2006; Kläusler et al. 2014; Vieira Rocha et al. 2018). The effect of these natural characteristics on the mechanical properties of wood has been significantly reduced by the application of wood glueing technologies: cross laminated timber (CLT), glued laminated timber (GLT), and laminated veneer lumber (LVL). A major improvement in the properties that reduce the value of wood is a result of the advanced process of glued wood production. Among others production line includes: sawing raw material, drying, planing, sorting, glueing, and re-machining (for GLT and CLT). The last one is the milling/planing process of the already glued material. The final machining operation provides the final dimensions with the required accuracy and expected surface quality (Wang et al. 2015; Christovasilis et al. 2016). In the manufacturing process of glulam (GLT, CLT), the glue used has a significant effect on tool wear and increases the cutting force (Bustos et al. 2010; Kläusler et al. 2014; Porankiewicz et al. 2014; Dobrzynski et al. 2019). The question is how can this effect be reduced?

The use of machining fluids in primary wood sawing processes is an industrial practice, especially for log band sawing processes. The main purpose of using machining fluids is to reduce the coefficient of friction, but also to prevent chips, sawdust, and resins from sticking to the cutting blades (Web-Source 1 (2022), Web-Source 2 (2022)). Stanovský et al. (2013) showed that oil lubrication of tool blades during the chain sawing process significantly reduced the temperature of the cutting process and tool wear by reducing the coefficient of friction. The use of similar machining fluids in the final processing of glued wood would probably reduce the phenomenon of adhesive sticking to cutting blades and their wear (Dobrzynski et al. 2019). However, they could negatively affect the properties of the machined wood surface, especially causing a change in colour, chemical compositions, and physical properties. In the case of blade lubrication used during pre-sawing wood processes (harvesting process—chain saw; sawing of log—band saw), the effect of machining fluid on the machined surface is not important, as these surfaces will be repeatedly machined and the effects will be removed during the subsequent manufacturing processes. Significant colour changes induced by thermal treatments (drying, steaming) take place at a small depth (around 2 mm) from the surface of treated wood, as shown by Konopka et al. (2021). However, for final machining operations, the use of machining fluids can affect the physical and chemical properties of the machined surface. Therefore, use of these fluids is not allowed in the secondary wood machining operations where the final surface of

wooden element is generated. The chemical and physical changes induced by the use of the machining fluid can affect the aesthetics of the product and the properties necessary for subsequent manufacturing steps, such as absorption during the painting process.

Colour is one of the most important characteristics of wood, which describes its aesthetic qualities relevant to the user (Forsthuber and Grüll 2018). Changes in wood colour described using the CIELab system (ISO 11664-2 (2007); ISO 11664-4 (2019)) are used to observe changes that occur as a result of various wood processing operations in the production of a wood product, e.g. drying (Cividini et al. 2007; Baranski et al. 2020), steaming (Tolvaj, et al. 2012; Geffert et al. 2017; Dzurenda 2022), thermal modification (Dagbro et al. 2010; Timar et al. 2016), and chemical modification (Bi et al. 2021). The various wood treatment/modification processes also cause changes in the chemical composition of the wood. Changes in the chemical composition can be analysed successfully using infrared spectroscopy (IR). Bader et al. (2020) used Fourier transform infrared spectroscopy (FTIR) to analyse chemical changes in wood induced by steaming and longitudinal compression. Chemical changes induced by heat treatment were analysed using near infrared spectroscopy by Sandak et al. (2016). Hofmann et al. (2022) applied FTIR analysis to monitor chemical changes of steamed wood of different species during short-term photodegradation. Varga et al. (2020) used IR spectroscopy to analyse the photodegradation of hardwood species and monitor water leaching from them. Broda and Popescu (2019) also used FTIR spectroscopy for comparative analysis of the natural decay of archaeological oak wood and artificial degradation processes.

The colour of wood also changes as a result of weathering (Jebrane et al. 2017) or light exposure (Calienzo et al. 2014). The colour analysis of wood can be used as a tool to identify specific wood characteristics (Klement and Vilkovská 2019). Colour and changes in colour are used as indicators of the quality of the wood processing performed (Torniainen et al. 2021) and as a tool to predict mechanical properties (Nasir et al. 2021). Moreover, different types of infrared spectroscopy (FTIR and NIR) have been applied to estimate the physical and mechanical properties of wood by Sandak et al. (2015). Kwasniewska-Sip et al. (2021) used FTIR spectroscopy to characterise the interaction between caffeine and Scots pine (*Pinus sylvestris* L.) wood and assess the stability of the alkaloid molecule in lignocellulosic material.

Studies on the analysis of colour and/or chemical changes as a result of the machining fluid on wood have not been reported in the available literature thus far. This is not surprising, as there are also no published studies in the available literature related to the application of machining fluids to the final machining step of wood, especially glulam. The aim of the conducted research was to analyse the changes

in colour and chemical composition occurring on the surface of machined Scots pine wood (*Pinus sylvestris* L.), as a result of the machining fluid. These tests are aimed at answering whether standard machining fluids dedicated to primary woodworking can also be used in the final machining processes of wooden products, especially glulam, without adverse consequences such as changes in colour and chemical composition. To the best of our knowledge this is a pioneering approach to final machining process of wood and glulam.

2 Materials and methods

2.1 Material and sample preparation process

The study was carried out on Scots pine wood (*Pinus sylvestris* L.) harvested from the Pomeranian region of Poland. Pine wood was chosen because it is the most popular in the timber industry in most of Europe, including for glulam production. Wood samples for analyses were prepared from 7 different logs. The logs were sawn for timber beams in a sawmill and then dried in an industrial kiln dryer to a moisture content (MC) of about 12%. One part of the beam was used to determine the density of the samples. Density was determined as the weight of wood divided by the volume of the sample in an oven-dry condition. The other parts of the beams were planed to 50 mm × 50 mm dimensions and cut to a length of 600 mm. One sample with final dimensions of 50 mm × 50 mm × 500 mm (respectively H–height × W–width × L–length) was prepared from each log. The obtained beams were stored in laboratory room and conditioned 24 h before the experiment under the conditions: temperature 20 °C (T) and 60% relative humidity (RH) in order to maintain MC at a constant value 12%.

The structural properties of the analysed wood samples are shown in Table 1.

Finally, the beams were sawn to 4 mm thick lamellae on the frame sawing machine PRW15M with elliptical tooth trajectory and a hybrid dynamically balanced driving system (Wasielewski and Orłowski 2002). In the machining process, machine settings were applied, which are shown in Table 2. The freshly machined surface of one lamella from each beam was subjected to analysis of the effect of machining fluids on colour changes.

2.2 Machining fluid and application process

The analysed machining fluid is a mixture of different fractions of heavy petroleum oil with a boiling point in the range

Table 2 Tool and machine tool data

Name of parameter	Symbol (unit)	Value
Frame sawing machine PRW15M		
Number of strokes of the saw frame per min	n_F (min ⁻¹)	685
Number of saws in the gang	m (–)	5
Average cutting speed	v_c (m·s ⁻¹)	3.69
Average feed speed	v_f (m·min ⁻¹)	0.92
Feed per tooth	f_z (mm)	0.11
Saw frame stroke	H_F (mm)	162
Tension stresses of saw blades in the gang	σ_N (MPa)	300
Saw blade (sharp, with stellite® tipped teeth)		
Kerf width (overall set)	S_i (mm)	2
Saw blade thickness	s (mm)	0.9
Free length of the saw blade	L_0 (mm)	318
Blade width	b (mm)	30
Tooth pitch	P (mm)	13
Tool side rake angle	γ_f (°)	9
Tool side clearance angle	α_f (°)	14

Table 1 Selected properties of analysed pine wood samples

Sample ID	Density of oven-dry pine wood ρ , kg·m ⁻³	Moisture content MC, %	Average width of the annual rings WAR, mm	Average width of the late-wood in annual ring LW, mm	Average width of the early-wood in annual ring EW, mm
S1	487.05	7.90	1.05	0.30	0.75
S2	625.71	10.30	1.81	0.73	1.09
S3	618.86	12.80	2.27	1.16	1.11
S4	453.23	8.60	4.56	0.67	3.89
S5	574.67	12.30	2.52	1.06	1.46
S6	536.34	12.40	2.12	0.40	1.72
S7	542.23	12.20	2.02	0.44	1.58
Average value	548.30	10.93	2.33	0.68	1.66
Standard deviation	64.08	2.01	1.08	0.33	1.04

Average values for the whole group of samples are in bold

of 155–217 °C (60–80% m/m), aromatic hydrocarbons with carbon numbers predominantly in C8–C10 and boiling point in the 135–210 °C (10–30% m/m) range, and white mineral oil with viscosity at 40 °C (10–30% m/m) in the range of 14.2–17.0 mPa·s. It did not contain silicone and wax. The density of the used machining fluid was 0.794 g/ml at 20 °C. The machining fluid was applied to the lamella by using a nozzle with a hand pump. A volume of 1 ml of machining fluid was applied evenly over the whole analysed wood surface $A_a = 4000 \text{ mm}^2$ in sprayed form (Fig. 1).

2.3 Methodology for measuring colour parameters

Changes in wood colour were measured based on the three-axis CIELab system recommended by CIE (Commission Internationale de l'Eclairage) and according to ISO 11664-2 and ISO 11664-4 standards (Baranski et al. 2020; Konopka et al. 2021). The main colour parameters (L^* , a^* , b^*) for each sample were measured using Colour Reader CR-10 (Konica Minolta, Inc., Tokyo, Japan). The standard illuminant was D65 and viewing angle 10°. Lightness (L^*) was measured directly on the samples, while colour chroma (C_{ab}^*), colour saturation (S_{ab}^*), and colour hue (h°) were determined from the measured values of the L^* and two other parameters a^* and b^* . The colour parameters for each sample were measured in 4 stages. The first stage was a reference measurement of the colour parameters on the machined surface of the samples (lamellae). The next three stages measured the colour parameters after the machining fluid had already been applied to the analysed wood surface in the following time frame: immediately after applying the machining fluid, 1 h after applying the machining fluid, and 24 h after applying the machining fluid to the wood surface. The 24-h analysis period adopted was chosen based on the experience from production processes in factories making glulam window and door frames. In these plants, the production flow is realised continuously in line and, from the final machining of the frame parts, through the assembly of the full frame, to the painting and lacquering of the full window frame, the process takes no longer than 24 h.

At each stage, 5 measurements were carried out for each sample. The overall colour difference was determined by using the parameter ΔE^* , as follows:

$$\Delta E^* = \sqrt{(L_2^* - L_1^*)^2 + (a_2^* - a_1^*)^2 + (b_2^* - b_1^*)^2} \quad (-) \quad (1)$$

where L_1^* , a_1^* , b_1^* are the values of colour spectra prior to the treatment process, and L_2^* , a_2^* , b_2^* are the values of colour spectra after the treatment process. The colour changes were assessed according to the scale proposed by Cividini et al. (2007), as follows:

$\Delta E^* < 0.2$: invisible colour change.

$2 > \Delta E^* > 0.2$: slight change in colour.

$3 > \Delta E^* > 2$: colour change visible with high quality screen.

$6 > \Delta E^* > 3$: colour changes visible with the medium quality screen.

$12 > \Delta E^* > 6$: strong colour change.

$\Delta E^* > 12$: different colour.

Colour chroma (C_{ab}^*) was also analysed. This parameter refers to the intensity of the colour and can also be defined as the bandwidth of the light generated from the source. Colour chroma (C_{ab}^*) was determined as follows:

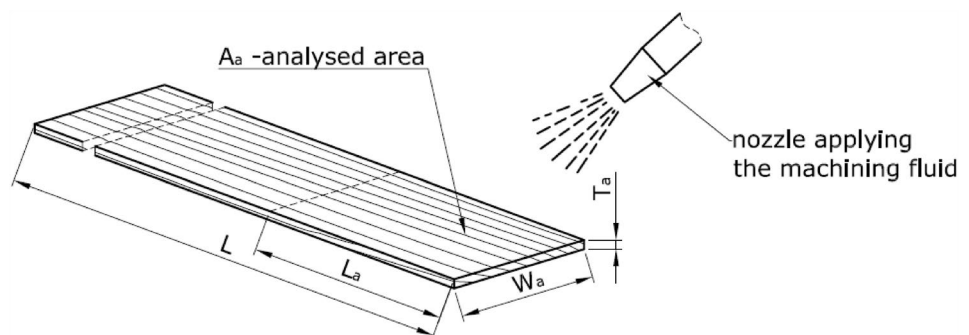
$$C_{ab}^* = \sqrt{a^{*2} + b^{*2}} \quad (-) \quad (2)$$

Other important parameters such as colour saturation (S_{ab}^*) and colour hue (h°) were also analysed. The colour saturation parameter can be estimated by combining the light intensity and its distribution in the spectrum at different wavelengths, as follows:

$$S_{ab}^* = \frac{C_{ab}^*}{\sqrt{C_{ab}^{*2} + L^{*2}}} \times 100(\%) \quad (3)$$

The colour hue value often corresponds to the angular position around a central point in the colour space coordinate system (Klement and Vilkovská 2019; Konopka et al. 2021) and can be determined as follows:

Fig. 1 Process of applying machining fluid on wood lamella, where: A_a analysed area, L_a length, W_a width of the analysed area, T_a thickness, and L length of the analysed lamella



$$h^{\circ} = \tan^{-1} \frac{b^{*}}{a^{*}} (^{\circ}) \quad (4)$$

Samples between measurements were stored under constant climatic conditions and without access to UV radiation.

2.4 Attenuated total reflectance Fourier transform infrared spectroscopy (ATR FTIR)

The spectra of native pine wood, machining fluid, and wood with partially evaporated machining fluid were measured. Sections of 0.7 ± 0.15 mm thickness were cut from both native pine wood and wood wetted with machining fluid, and their ATR FTIR spectra were recorded. In the case of ATR FTIR test the spectra for wetted wood with machining fluid were recorded after around 1 h and after 24 h. This difference in testing colour changes was due to the limited possibility of conducting the test in similar time periods. The ATR FTIR spectra of samples were recorded on Nicolet 8700 spectrophotometer (Thermo Electron Scientific Inc., Waltham, MA), using a Golden Gate ATR accessory (Specac) equipped with a single-reflection diamond crystal. The temperature during measurements was kept at 25 ± 0.1 °C using an electronic temperature controller (Specac). For each spectrum, 128 scans were collected in the range of 500 to 4000 cm^{-1} , with resolution of 4 cm^{-1} . For each sample, at least five replicate spectra were recorded to assess precision and ensure the reproducibility of each sample. The presented results are average values.

2.5 Statistical analysis

The results of the obtained values of the colour parameters were subjected to statistical analyses. An analysis of variance (ANOVA) was performed on the results, which was used to determine the significance in differences between colour parameters measured for the surfaces of standard wood (without applying the machining fluid) and wood surfaces 24 h after the application of the machining fluid (Sachs 1984).

3 Results and discussion

The changes in basic colour parameters, such as lightness (L^*) and colour chroma (C_{ab}^*), caused by the application of the machining fluid to pine wood are shown in Figs. 2 and 3. In Fig. 2, it is noticeable that the lightness values decreased dramatically, immediately after applying the machining fluid to the wood surface, but started to increase with time; however, after 24 h they were still statistically significantly different from the initial values (Table 3). In the case of the chroma parameter (Fig. 3), there was a strong increase

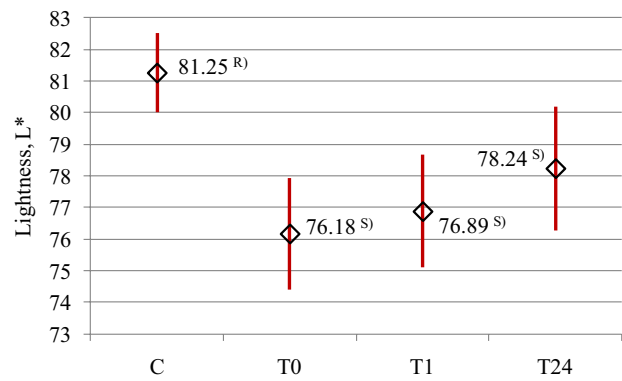


Fig. 2 Changes in the value of the colour parameter—lightness L^* of pine wood depending on the application of the machining fluid and the time after its application. C—values measured immediately before applying the machining fluid on wood; T0—values measured immediately after applying the machining fluid on wood; T1—values measured 1 h after applying the machining fluid on wood; T24—values measured 24 h after applying the machining fluid on wood. Average values (diamonds) with standard deviations (vertical lines). ^R—reference value; ^S—values statistically different from the reference value at $\alpha=0.05$

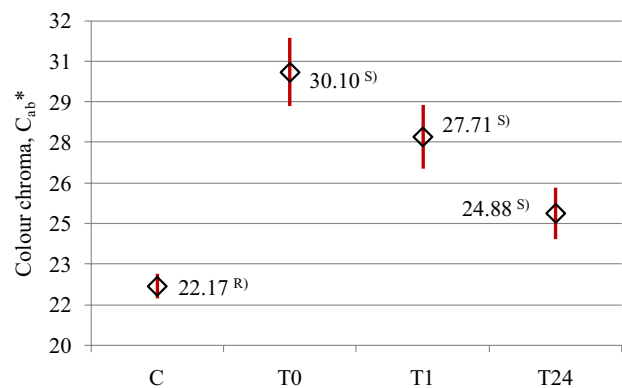


Fig. 3 Changes in the value of the colour parameter—chroma C_{ab}^* of pine wood depending on the application of the machining fluid and the time after its application. Average values (diamonds) with standard deviations (vertical lines). ^R—reference value; ^S—values statistically different from the reference value at $\alpha=0.05$ (for abbreviations see Fig. 2)

in values following immediate application of the machining fluid to the wood surface. Thereafter, they gradually decreased; however, despite a fairly long period (24 h), they were still statistically significantly different from the values for wood that was not subjected to the application of machining fluid (Table 3).

A similar pattern of change, as in the case of the chroma parameter, can be observed for the colour saturation parameter S_{ab}^* (Fig. 4). After the machining fluid is applied to the wood surface, the colour saturation increases strongly, but decreases with time. However, after 24 h, the difference in the colour saturation values remained statistically significant

Table 3 The significance of differences between colour parameters values obtained for the wood surfaces before applying machining fluid (control) and 24 h after applying the machining fluid (ANOVA) ($\alpha=0.05$, $p<0.05$)

Source	DF	Adj SS	Adj MS	F-Value	p-Value	F-Critical
Colour lightness L^*						
Between groups	1	31.801	31.801	11.719	$5.05 \times 10^{-3 S)}$	4.747
Within groups	12	32.562	2.714			
Total	13	64.363				
Colour chroma C_{ab}^*						
Between groups	1	25.573	25.5732	45.873	$1.98 \times 10^{-5 S)}$	4.747
Within groups	12	6.690	0.557482			
Total	13	32.263				
Colour saturation S_{ab}^*						
Between groups	1	55.617	55.617	48.755	$1.5 \times 10^{-5 S)}$	4.747
Within groups	12	13.689	1.1408			
Total	13	69.306				
Colour hue h°						
Between groups	1	11.266	11.266	0.898	$3.62 \times 10^{-1 NS)}$	4.747
Within groups	12	150.558	12.547			
Total	13	161.824				
Total colour changes ΔE^*						
Between groups	1	60.782	60.782	84.009	$9.1 \times 10^{-7 S)}$	4.747
Within groups	12	8.682	0.724			
Total	13	69.464				

^{S)} values statistically different from the reference value at $\alpha=0.05$

^{NS)} values not statistically different from the reference value at $\alpha=0.05$

DF degree of freedom, *Adj. SS* adjusted sums of squares, *Adj. MS* adjusted mean squares

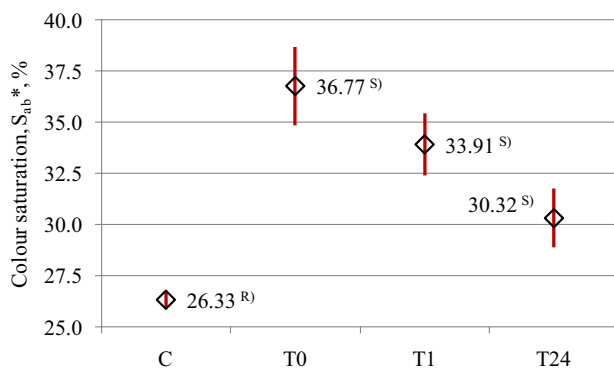


Fig. 4 Changes in the value of the colour parameter—saturation S_{ab}^* of pine wood depending on the application of the machining fluid and the time after its application. Average values (diamonds) with standard deviations (vertical lines). ^{R)}—reference value; ^{S)}—values statistically different from the reference value at $\alpha=0.05$ (for abbreviations see Fig. 2)

from the values determined for the wood before applying the machining fluid (Table 3).

Thus, it can be seen that the application of the treatment liquid to pine wood resulted in a slight darkening of the wood, an increase in colour intensity, and saturation. It can also be assumed that these changes are long-lasting, as significant differences persisted after 24 h with respect to wood

not subjected to the machining fluid application (Table 3). The observed decrease in values over time is probably due to the evaporation of some of the volatile components of the machining fluid, thus reducing its effects on the colour of the wood. However, this is not a strongly intense process, which means that the changes last longer. It can be assumed that over time most of the hydrocarbons that are in the machining fluid will evaporate, but during production processes and next exploitation then colour changes will also occur as a result of normal aging of wood and/or solar radiation (Laskowska 2020; Dudiak et al. 2022). Therefore, measuring the evaporation of hydrocarbons from wood by measuring colour changes would be difficult, because the colour changes would be significantly affected by changes in the chemical composition related to solar radiation (Sandak et al. 2021) as well as the evaporation of hydrocarbons contained in the machining fluid.

Machining fluid does not affect the hue at all, as can be seen in Fig. 5 and Table 3.

However, the values of the total colour change parameter ΔE^* show a similar trend (Fig. 6) to that of chroma C_{ab}^* (Fig. 3) and saturation S_{ab}^* (Fig. 4). The parameter values are statistically different from the reference values (Table 3). Also, on the scale proposed by Cividini et al. (2007), the differences are significant, as they have a mean value of 4.17 which falls in the range $6 > \Delta E^* > 3$ and means that the

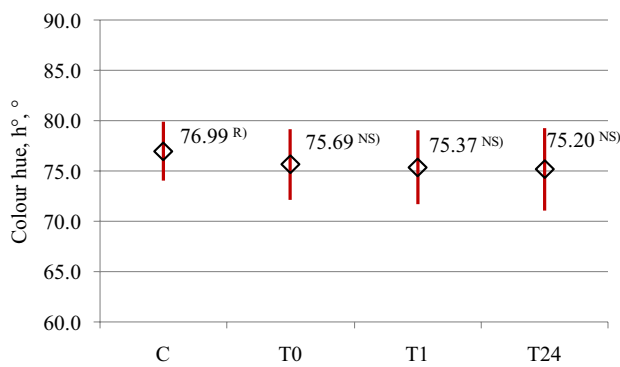


Fig. 5 Changes in the value of the colour parameter—hue h° of pine wood depending on the application of the machining fluid and the time after its application. Average values (diamonds) with standard deviations (vertical lines). ^R—reference value; ^S—values statistically different from the reference value at $\alpha=0.05$ (for abbreviations see Fig. 2)

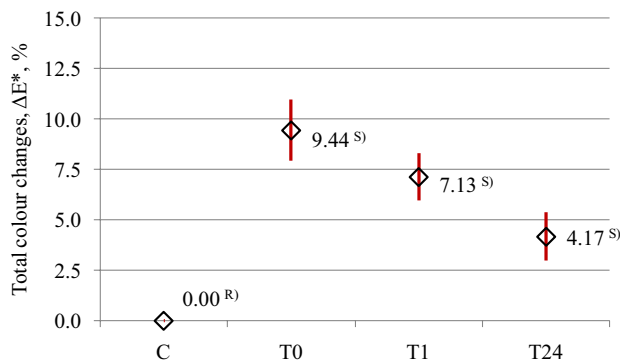


Fig. 6 Changes in the value of the parameter of total colour changes ΔE^* for pine wood depending on the application of the machining fluid and the time after its application. Average values (diamonds) with standard deviations (vertical lines). ^R—reference value; ^S—values statistically different from the reference value at $\alpha=0.05$ (for abbreviations see Fig. 2)

changes in the colour are visible with the average quality of the filter.

The visual changes in the colour of pine wood caused by the application of the standard processing fluid are shown in Table 4 along with the difference in the values of the measured colour parameters in relation to the reference surface, which was the wood surface before the application of the machining fluid.

The spectrum of the machining fluid resembles that of n-hexane (Fig. 7) (Mirghani and Man 2003); hence, it can be assumed that hexane is the basic component of the machining fluid. This spectrum shows absorption bands at 2956, 2923, 2872, and 2853 cm^{-1} which correspond to the stretching vibrations of C-H (ν_{CH}), and absorption bands at 1459


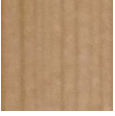

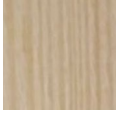
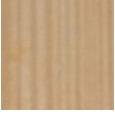















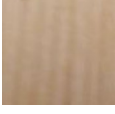
and 1378 cm^{-1} , which are characteristic of the C-H bending vibrations (δ_{CH}).

The pine wood spectrum shows all the characteristic bands for cellulose, hemicellulose, and lignin that have been widely reported in the available literature. The broad band at the 3600–3100 cm^{-1} region corresponds to the stretching vibrations of the hydroxyl groups (ν_{OH}) (Esteves et al. 2013; Schwanninger et al. 2004), and the band in the 3000–2800 cm^{-1} range, is characteristic of symmetric and asymmetric ν_{CH} in $-\text{CH}-$, $-\text{CH}_2$ and $-\text{CH}_3$ groups (Esteves et al. 2013; Schwanninger et al. 2004). Absorption bands observed in the 1655–1730 cm^{-1} range are attributed to $\nu_{\text{C=O}}$ in carbonyl moieties: a small band with a maximum at 1730 cm^{-1} indicates $\nu_{\text{C=O}}$ of acetyl, carboxyl, unconjugated ketones, or ester groups (Schwanninger et al. 2004), while the band at 1693 cm^{-1} indicates conjugated aldehydes and carboxylic acids (Esteves et al. 2013; Schwanninger et al. 2004). The bands in the 1600–1420 cm^{-1} region are assigned to structures characteristic for lignin, i.e. the vibrations of bonds in aromatic rings (Esteves et al. 2013; Shi et al. 2012; Schwanninger et al. 2004; Traore et al. 2018). Furthermore, the spectrum of native pine wood showed characteristic absorption peaks at 1370 and 1270 cm^{-1} , corresponding to hydroxyl groups associated with aliphatic and aromatic carbon, respectively (Esteves et al. 2013; Shi et al. 2012; Schwanninger et al. 2004; Traore et al. 2018). The band in the 1163–985 cm^{-1} range is a saccharide band: the one visible at 1163 cm^{-1} is assigned to asymmetric $\nu_{\text{O-C-O}}$ both in the crystalline cellulose I, cellulose II, and hemicellulose (Shi et al. 2012; Traore et al. 2018), and those visible at 1109 and 1057 cm^{-1} are attributed to $\delta_{\text{C-OH}}$ (Esteves et al. 2013; Shi et al. 2012; Schwanninger et al. 2004; Traore et al. 2018). The band at 897 cm^{-1} is characteristic of asymmetric out-of-phase stretching vibration in pyranose ring (Shi et al. 2012; Esteves et al. 2013; Schwanninger et al. 2004).

The spectrum of wood after wetting with machining fluid is the result of the spectra of native wood and hexane originating from machining fluid. The spectrum shows bands characteristic for native wood and those characteristic for hexane.

The difference in the spectrum of the wood wetted with machining fluid (both after 1 h and 24 h), in relation to that of the native pine wood can be seen in a very slight change in shape of the 3600–3100 cm^{-1} band, which can be attributed to ν_{OH} vibrations. This change manifests in a shift of the band maximum towards lower wavenumbers. This may indicate an increase in the importance of intramolecular hydrogen bonds in cellulose in favor of intermolecular bonds (Janardhnan and Sain 2011; Poletto et al. 2012; Popescu et al. 2011; Zhu Ryberg et al. 2011) as a result of using machining fluid and may be explained as a hydrophobic effect occurring under the influence of hydrophobic fluid.

Table 4 Visual assessment of the colour changes in pine wood caused by application of the standard processing fluid

Sample symbol	Control		T0		T24	
S1		L* = 80.26 ± 0.21 a* = 6.22 ± 0.13 b* = 20.82 ± 0.19		ΔL* = -5.90 ± 0.25 Δa* = 3.82 ± 0.26 Δb* = 8.50 ± 0.23		ΔL* = -3.28 ± 0.34 Δa* = 1.80 ± 0.24 Δb* = 0.88 ± 0.33
S2		L* = 80.50 ± 0.26 a* = 4.50 ± 0.19 b* = 22.08 ± 0.32		ΔL* = -5.58 ± 0.33 Δa* = 2.44 ± 0.15 Δb* = 7.74 ± 0.25		ΔL* = -2.78 ± 0.08 Δa* = 1.04 ± 0.09 Δb* = 2.48 ± 0.45
S3		L* = 82.52 ± 0.44 a* = 4.12 ± 0.27 b* = 21.50 ± 0.33		ΔL* = -4.10 ± 0.78 Δa* = 1.42 ± 0.50 Δb* = 5.76 ± 0.54		ΔL* = -2.76 ± 0.61 Δa* = 0.74 ± 0.30 Δb* = 2.98 ± 0.37
S4		L* = 80.16 ± 0.09 a* = 6.36 ± 0.05 b* = 20.74 ± 0.11		ΔL* = -5.96 ± 0.32 Δa* = 3.96 ± 0.15 Δb* = 8.96 ± 0.34		ΔL* = -3.82 ± 0.27 Δa* = 2.52 ± 0.11 Δb* = 3.24 ± 0.49
S5		L* = 80.10 ± 0.83 a* = 5.36 ± 0.31 b* = 21.40 ± 0.23		ΔL* = -4.04 ± 2.17 Δa* = 2.18 ± 0.44 Δb* = 6.78 ± 0.29		ΔL* = -4.16 ± 1.06 Δa* = 1.84 ± 0.44 Δb* = 3.76 ± 0.49
S6		L* = 82.58 ± 0.13 a* = 3.98 ± 0.16 b* = 22.10 ± 0.53		ΔL* = -4.46 ± 0.27 Δa* = 1.80 ± 0.19 Δb* = 7.22 ± 0.58		ΔL* = -2.36 ± 0.17 Δa* = 0.96 ± 0.26 Δb* = 2.04 ± 0.47
S7		L* = 82.66 ± 0.05 a* = 4.26 ± 0.05 b* = 22.46 ± 0.78		ΔL* = -5.48 ± 0.41 Δa* = 1.82 ± 0.16 Δb* = 7.74 ± 0.74		ΔL* = -1.94 ± 0.30 Δa* = 0.64 ± 0.17 Δb* = 1.54 ± 1.01

Average values of parameters and colour changes with standard deviations

All colour changes are shown relative to the reference surface, which is the surface before the fluid was applied. Control—the colour parameters were measured immediately before applying the machining fluid to the wood surface; T0—the colour parameters were measured immediately after applying the machining fluid to the wood surface; T24—the colour parameters were measured 24 h after the machining fluid was applied to the wood surface

The most visible change in the spectrum of wetted wood compared to the native one is the disappearance of a medium-intense narrow band at 1693 cm⁻¹. This band is only visible in the spectrum of the native pine wood sample and is completely missing in all samples of wetted wood. According to Funda et al. 2020, the band at 1693 cm⁻¹ is characteristic for *extractives*, i.e. low-molecular-weight organic and inorganic compounds found in young wood. Carrion-Prieto et al. 2018 consider this band to be characteristic of ν_{C-O} in terpenic oxo groups of diterpenes. As diterpenes are volatile compounds (Najda 2015; Miller et al. 2005), those present in the native wood probably dissolved in the machining fluid and evaporated with it. Although the spectrum of diterpenes, chemically heterogeneous compounds, has many characteristic absorption bands (Costa et al. 2020), unfortunately most of them overlap

with the bands observed in the spectrum of wood; hence, they are not clearly distinguishable.

In the spectrum of wood wetted with machining fluid, a new band appears at 1377 cm⁻¹. This band is related to the presence of this fluid in the wood, and it proves that the fluid did not evaporate from the wood either after 1 or 24 h.

The band at 1452 cm⁻¹ appearing in the spectrum of native pine is shifted towards higher wavenumbers after wetting the wood with the treatment liquid. This is because in wetted wood it is overlaid with the band characteristic for the machining fluid at 1458 cm⁻¹.

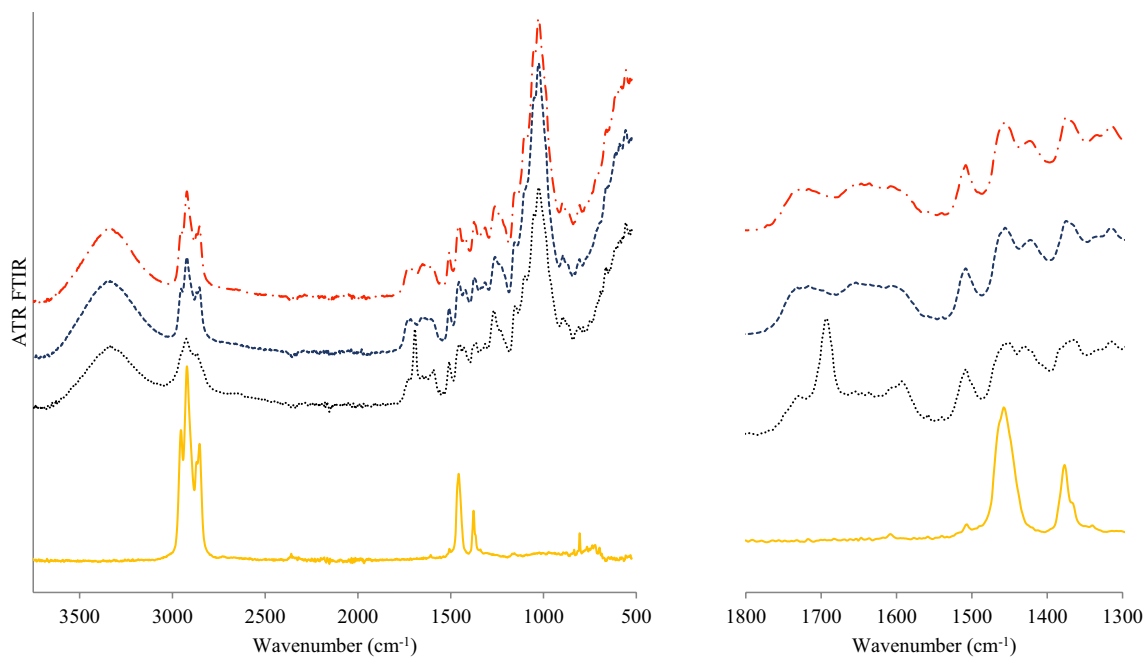


Fig. 7 FTIR spectra of machining fluid (—), native pine wood sample (.....) and pine wood sample wetted with machining fluid, after 1 h (---) and 24 h (-.-.-)

4 Conclusion

The use of machining fluid is one of the methods available to reduce friction in the cutting process of wood. In the case of solid wood, they are mainly used to reduce the encapsulation of cutter blades, by resins contained in the wood during primary machining processes. These fluids could also be used in the final machining processes of glued laminated timber products to reduce the exertion of glue on the cutting tool blades. However, in this case, they should not induce chemical and physical changes on the final machined surface. On the basis of the carried out experimental tests and analysis of obtained results, it can be concluded that:

- Standard machining fluids dedicated to wood processing significantly cause a change in the colour of the machined surface.
- Changes in the colour of pine wood induced by the use of standard machining fluids decrease over time; however, significant differences from the reference values remain after 24 h.
- Changes in the colour of pine wood caused by the use of machining fluids generally result in a slight darkening and an increase in the saturation and intensity of the colour of wood surface. However, these changes of saturation can be not regular and only locally, which may not be an advantage for consumers.
- The bands in the spectrum of the wood wetted with machining fluid are the overlapped bands of wood and

the machining fluid, which shows that there were no chemical changes. Although the fluid does not significantly affect the wood chemical composition, it can interfere with later processing steps, for example adhesion of paints or surface impregnation of wood.

- To reduce the effect of the machining fluid on the colour of the wood, its composition should be changed to allow and/or accelerate the evaporation of their components from the surface of the machined wood.
- Non-evaporated hydrocarbons from the machining fluid can affect further manufacturing processes of wood components, e.g. by affecting the coating process, as well as bonding with the glue analysed surface.

Acknowledgements Financial support for this study from Gdansk University of Technology by the DEC-15/2021/IDUB/I.3.3 grant under the Argentum Triggering Research Grants—‘Excellence Initiative—Research University’ program and by the DEC-1/2020/IDUB/II.1 grant under the Hydrogenium Supporting Membership In International Networks—‘Excellence Initiative—Research University’ program is gratefully acknowledged. Authors would like to acknowledge Ms Joanna Kurach and Würth Polska Sp. z o.o. for their support of the experiment.

Author contributions DC and AS wrote the main manuscript text; DC and AS prepared figures; DC and KO carried out a colour analysis; AS, HS and SM carried out a chemical composition analyses; JS verified the results and provided supervision; All authors reviewed and modified the manuscript

Declarations

Conflict of interest The authors declare no competing interests.

Open Access This article is licensed under a Creative Commons Attribution 4.0 International License, which permits use, sharing, adaptation, distribution and reproduction in any medium or format, as long as you give appropriate credit to the original author(s) and the source, provide a link to the Creative Commons licence, and indicate if changes were made. The images or other third party material in this article are included in the article's Creative Commons licence, unless indicated otherwise in a credit line to the material. If material is not included in the article's Creative Commons licence and your intended use is not permitted by statutory regulation or exceeds the permitted use, you will need to obtain permission directly from the copyright holder. To view a copy of this licence, visit <http://creativecommons.org/licenses/by/4.0/>.

References

- As N, Goker Y, Dundar T (2006) Effect of knots on the physical and mechanical properties of Scots pine (*Pinus Sylvestris* L.). *Wood Research* 51(3):51–58
- Asdrubali F, Ferracuti B, Lombardi L, Guattari C, Evangelisti L, Grazieschi G (2017) A review of structural, thermo-physical, acoustical, and environmental properties of wooden materials for building applications. *Build Environ* 114:307–332. <https://doi.org/10.1016/j.buildenv.2016.12.033>
- Bader M, Nemeth R, Sandak J, Sandak A (2020) FTIR analysis of chemical changes in wood induced by steaming and longitudinal compression. *Cellulose* 27:6811–6829. <https://doi.org/10.1007/s10570-020-03131-8>
- Baranski J, Konopka A, Vilkovská T, Klement I, Vilkovský P (2020) Deformation and surface color changes of beech and oak wood lamellas resulting from the drying process. *Bioresources* 15(4):8965–8980. <https://doi.org/10.15376/biores.15.4.8965-8980>
- Bi Z, Yuan J, Morrell JJ, Yan L (2021) Effects of extracts on the colour of thermally modified *Populus tomentosa* Carr. *Wood Sci Technol* 55:1075–1090. <https://doi.org/10.1007/s00226-021-01304-7>
- Broda M, Popescu C-M (2019) Natural decay of archaeological oak wood versus artificial degradation processes — An FT-IR spectroscopy and X-ray diffraction study. *Spectrochim Acta Part A Mol Biomol Spectrosc* 209:280–287. <https://doi.org/10.1016/j.saa.2018.10.057>
- Brunet-Navarro P, Jochheim H, Cardellini G, Richter K, Muys B (2021) Climate mitigation by energy and material substitution of wood products has an expiry date. *J Clean Prod* 303:127026. <https://doi.org/10.1016/j.jclepro.2021.127026>
- Bustos CA, Moya CL, Lisperguer JM, Viveros EM (2010) Effect of knife wear on the gluability of planed surfaces of radiata pine. *Wood Fiber Sci* 42(2):185–191
- Calienzo L, Lo Monaco A, Pelosi C, Picchio R (2014) Colour and chemical changes on photodegraded beech wood with or without red heartwood. *Wood Sci Technol* 48:1167–1180. <https://doi.org/10.1007/s00226-014-0670-z>
- Carrión-Prieto P, Martín-Gil J, Fernández-Coppel IA, Ruíz-Potosme NM, Martín-Ramos P (2018) Physicochemical studies of Siberian pine (*Pinus sibirica*) derived chewing gum. *Trends Phytochem Res* 2(2):119–124
- Christovasilis IP, Brunetti M, Follera M, Nocetti M, Vassallo D (2016) Evaluation of the mechanical properties of cross laminated timber with elementary beam theories. *Constr Build Mater* 122:202–213. <https://doi.org/10.1016/j.conbuildmat.2016.06.082>
- Cividini R, Travan L, Allegretti O (2007) White beech: A tricky problem in drying process. *Proceedings of 7th ISCHP (International Scientific Conference on Hardwood Processing)*, 24–26 September 2007, Quebec City, Canada
- Costa EV, Sampaio MF, Menezes LR, Dutra LM, Costa CO, Pinheiro MLB, Koolen HH (2020) Diversity of the diterpenes in the leaves of *Xylopi laevigata* (Annonaceae) and their cytotoxicities. *Química Nova* 43:419–425. <https://doi.org/10.21577/0100-4042.20170504>
- Dagbro O, Torniainen P, Karlsson O, Morén T (2010) Colour responses from wood, thermally modified in superheated steam and pressurized steam atmospheres. *Wood Mat Sci Eng* 5(3–4):211–219. <https://doi.org/10.1080/17480272.2010.520739>
- Dobrzynski M, Orlowski KA, Biskup M (2019) Comparison of surface quality and tool-life of glulam window elements after planing. *Drvna Industrija* 70(1):7–18. <https://doi.org/10.5552/drind.2019.1741>
- Dudiak M, Dzurenda L, Kucerová V (2022) Effect of sunlight on the change in color of unsteamed and steamed beechwood with water steam. *Polymers* 14:1697. <https://doi.org/10.3390/polym14091697>
- Dzurenda L (2022) Range of color changes of beech wood in the steaming process. *BioResources* 17(1):1690–1702
- Esteves B, Velez Marques A, Domingos I, Pereira H (2013) Chemical changes of heat treated pine and eucalypt wood monitored by FTIR. *Maderas Ciencia y Tecnología* 15(2):245–258. <https://doi.org/10.4067/S0718-221X2013005000020>
- Forsthuber B, Grill G (2018) Prediction of wood surface discoloration for applications in the field of architecture. *Wood Sci Technol* 52:1093–1111. <https://doi.org/10.1007/s00226-018-1015-0>
- Funda T, Fundova I, Gorzsás A, Fries A, Wu HX (2020) Predicting the chemical composition of juvenile and mature woods in Scots pine (*Pinus sylvestris* L.) using FTIR spectroscopy. *Wood Sci Technol* 54(2):289–311. <https://doi.org/10.1007/s00226-020-01159-4>
- Geffert A, Výbohá E, Geffertová J (2017) Characterization of the changes of colour and some wood components on the surface of steamed beech wood. *Acta Facultatis Xylogiae Zvolen* 59(1):49–57. <https://doi.org/10.17423/afx.2017.59.1.05>
- Harris M (2012) Wood goes high-rise. *Eng Technol* 7(9):43–45. <https://doi.org/10.1049/et.2012.0902>
- Hassan OAB, Johansson C (2018) Glued laminated timber and steel beams: a comparative study of structural design, economic and environmental consequences. *J Eng Design Technol* 16(3):398–417. <https://doi.org/10.1108/JEDT-12-2017-0130>
- Himes A, Busby G (2020) Wood buildings as a climate solution. *Dev Built Environ* 4:100030. <https://doi.org/10.1016/j.dibe.2020.100030>
- Hofmann T, Tolvaj L, Visi-Rajczi E, Varga D (2022) Chemical changes of steamed timber during short-term photodegradation monitored by FTIR spectroscopy. *Eur J Wood Prod* 80:841–849. <https://doi.org/10.1007/s00107-022-01814-6>
- ISO 11664–2 (2007) Colorimetry-Part 2: CIE Standard Illuminants. International Organization for Standardization, Geneva
- ISO 11664–4 (2019) Colorimetry-Part 4: CIE 1976 L*a*b* Colour Space. International Organization for Standardization, Geneva
- Janardhnan S, Sain M (2011) Isolation of cellulose nanofibers: effect of biotreatment on hydrogen bonding network in wood fibers. *Int J Polym Sci*. <https://doi.org/10.1155/2011/279610>
- Jebrane M, Franke T, Terziev N, Panov D (2017) Natural weathering of Scots pine (*Pinus sylvestris* L.) wood treated with epoxidized linseed oil and methyltriethoxysilane. *Wood Mater Sci Eng* 12(4):220–227. <https://doi.org/10.1080/17480272.2016.1160954>
- Kläusler O, Rehm K, Elstermann F, Niemi P (2014) Influence of wood machining on tensile shear strength and wood failure percentage of one-component polyurethane bonded wooden joints after wetting. *Int Wood Prod J* 5(1):18–26. <https://doi.org/10.1179/2042645313Y.0000000039>
- Klement I, Vilkovská T (2019) Color characteristics of red false heartwood and mature wood of beech (*Fagus sylvatica* L.) determining

- by different chromacity coordinates. Sustainability 11(3):690. <https://doi.org/10.3390/su11030690>
- Konopka A, Chuchala D, Orlowski KA, Vilkovská T, Klement I (2021) The effect of beech wood (*Fagus sylvatica* L.) steaming process on the colour change versus depth of tested wood layer. Wood Mater Sci Eng 17(6):420–428. <https://doi.org/10.1080/17480272.2021.1942200>
- Kwasniewska-Sip P, Wozniak M, Jankowski W, Ratajczak I, Cofta G (2021) Chemical changes of wood treated with caffeine. Materials 14(3):497. <https://doi.org/10.3390/ma14030497>
- Laskowska A (2020) The influence of ultraviolet radiation on the colour of thermo-mechanically modified beech and oak wood. Maderas Cienc Tecnol 22(1):55–68. <https://doi.org/10.4067/S0718-221X2020005000106>
- Miller B, Madilao LL, Ralph S, Bohlmann J (2005) Insect-induced conifer defense. White pine weevil and methyl jasmonate induce traumatic resinosis, de novo formed volatile emissions, and accumulation of terpenoid synthase and putative octadecanoid pathway transcripts in Sitka spruce. Plant Physiol 137:369–382. <https://doi.org/10.1104/pp.104.050187>
- Mirghani MES, Che Man YB (2003) Determination of hexane residues in vegetable oils with FTIR spectroscopy. J Am Oil Chem Soc 80(7):619–623
- Najda A (2015) Plant volatile substances-essential oils. Episteme 27(2):65–77 (in Polish)
- Nasir V, Fathi H, Fallah A, Kazemirad S, Sassani F, Antov P (2021) Prediction of mechanical properties of artificially weatheredwood by color change and machine learning. Materials 14(21):6314. <https://doi.org/10.3390/ma14216314>
- Poletto M, Zattera AJ, Santana RM (2012) Structural differences between wood species: evidence from chemical composition, FTIR spectroscopy, and thermogravimetric analysis. J Appl Polym Sci 126(S1):E337–E344. <https://doi.org/10.1002/app.36991>
- Popescu MC, Popescu CM, Lisa G, Sakata Y (2011) Evaluation of morphological and chemical aspects of different wood species by spectroscopy and thermal methods. J Mol Struct 988(1–3):65–72. <https://doi.org/10.1016/j.molstruc.2010.12.004>
- Porankiewicz B, Józwiak K, Wiczorek D, Idzikowski I (2014) Specific wear on the rake face made of sintered carbide cutting edge during milling of laminated wood. Eur J Wood Prod 73(1):35–41. <https://doi.org/10.1007/s00107-014-0862-0>
- Ramage MH, Burrige H, Busse-Wicher M, Fereday G, Reynolds T, Shah DU, Wu G, Yu L, Fleming P, Densley-Tingley D, Allwood J, Dupree P, Linden PF, Scherman O (2017) The wood from the trees: The use of timber in construction. Renew Sustain Energy Rev 68(1):333–359. <https://doi.org/10.1016/j.rser.2016.09.107>
- Sachs L (1984) Applied Statistics. A Handbook of Techniques, 2nd edn. Springer, New York
- Sandak A, Sandak J, Riggio M (2015) Estimation of physical and mechanical properties of timber members in service by means of infrared spectroscopy. Constr Build Mater 101:1197–1205. <https://doi.org/10.1016/j.conbuildmat.2015.06.063>
- Sandak J, Sandak A, Allegretti O (2016) Chemical changes to woody polymers due to high-temperature thermal treatment assessed with near infrared spectroscopy. Near Infrared Spectrosc 24:555–562. <https://doi.org/10.1255/jnirs.1220>
- Sandak A, Sandak J, Noël M, Dimitriou A (2021) A method for accelerated natural weathering of wood subsurface and its multilevel characterization. Coatings 11(2):126. <https://doi.org/10.3390/coatings11020126>
- Schwanninger MJCR, Rodrigues JC, Pereira H, Hinterstoisser B (2004) Effects of short-time vibratory ball milling on the shape of FT-IR spectra of wood and cellulose. Vib Spectrosc 36(1):23–40. <https://doi.org/10.1016/j.vibspec.2004.02.003>
- Sekularac JI, Tovarovic JC, Sekularac N (2016) Application of wood as an element of façade cladding in construction and reconstruction of architectural objects to improve their energy efficiency. Energy Build 115:85–93. <https://doi.org/10.1016/j.enbuild.2015.03.047>
- Shi J, Xing D, Lia J (2012) FTIR studies of the changes in wood chemistry from wood forming tissue under inclined treatment. Energy Procedia 16:758–762. <https://doi.org/10.1016/j.egypro.2012.01.122>
- Stanovský M, Schürger J, Jankovský M, Messingerová V, Hnilica R, Kučera M (2013) The effect of lubricating oil on temperature of chainsaw cutting system. Croat J Forest Eng 34(1):83–90
- Tetty UYA, Doodoo A, Gustavsson L (2019) Carbon balances for a low energy apartment building with different structural frame materials. Energy Procedia 158:4254–4261
- Timar MC, Varodi A, Hacibektasoglu M, Campean M (2016) Color and FTIR analysis of chemical changes in beech wood (*Fagus sylvatica* L.) after light steaming and heat treatment in two different environments. Bioresources 11(4):8325–8343
- Tollefson J (2017) The wooden skyscrapers that could help to cool the planet. Nature 545:280–282. <https://doi.org/10.1038/545280a>
- Tolvaj L, Papp G, Varga D, Lang E (2012) Effect of steaming on the colour change of softwoods. BioResources 7(3):2799–2808
- Tornaiainen P, Jones D, Sandberg D (2021) Colour as a quality indicator for industrially manufactured ThermoWood®. Wood Mat Sci Eng 16(4):287–289. <https://doi.org/10.1080/17480272.2021.1958920>
- Traoré M, Kaal J, Martínez Cortizas A (2018) Differentiation between pine woods according to species and growing location using FTIR-ATR. Wood Sci Technol 52:487–504. <https://doi.org/10.1007/s00226-017-0967-9>
- Varga D, Tolvaj L, Molnar Z, Pasztory Z (2020) Leaching effect of water on photodegraded hardwood species monitored by IR spectroscopy. Wood Sci Technol 54:1407–1421. <https://doi.org/10.1007/s00226-020-01204-2>
- Vieira Rocha MF, Costa LR, Costa LJ, Caxito de Araújo AC, Dias Soares BC, Gherardi Hein PR (2018) Wood knots influence the modulus of elasticity and resistance to compression. Floresta e Ambiente 25(4):e20170906. <https://doi.org/10.1590/2179-8087.090617>
- Wang Z, Gong M, Chui Y-H (2015) Mechanical properties of laminated strand lumber and hybrid cross-laminated-timber. Constr Build Mater 101:622–627. <https://doi.org/10.1016/j.conbuildmat.2015.10.035>
- Wasielowski R, Orlowski K (2002) Hybrid dynamically balanced saw frame drive. Holz Roh Werkst 60(3):202–206
- Web-Source 1 <https://eshop.wurth.pl/Kategorie-produktow/Preparatoposlizgowy-do-drewna/31113008020101.cyid/3111.cgid/pl/PL/PLN/?CatalogCategoryRef=31113008020101%40WuerthGroup-Wuerth-3111&SelectedFilterAttribut=%255B%255D>. Accessed Oct 2022
- Web-Source 2 <https://www.wintersteiger.com/en/Woodtech/Flooring-furniture-and-boards/Product-range/Thin-cutting-sawing-machines/569-DSB-Twinhead-Pro-XM>. Accessed Oct 2022
- Wieruszewski M, Mazela B (2017) Cross laminated timber (CLT) as an alternative form of construction wood. Drvna Industrija 68(4):359–367. <https://doi.org/10.5552/drind.2017.1728>
- Wu X, Zhu J, Wang X (2021) A review on carbon reduction analysis during the design and manufacture of solid wood furniture. BioResources 16(3):6212–6230. <https://doi.org/10.15376/biores.16.3.6212-6230>
- Zhu Ryberg YZ, Edlund U, Albertsson AC (2011) Conceptual approach to renewable barrier film design based on wood hydrolysate. Biomacromol 12:1355–1362. <https://doi.org/10.1021/bm200128s>